Observation of two-dimensional nonlocal gap solitons

Per Dalgaard Rasmussen[1,2], Francis H. Bennet[1], Dragomir N. Neshev[1], Andrey A. Sukhorukov[1], Christian R. Rosberg[1], Wieslaw Krolikowski[1], Ole Bang[2], and Yuri S. Kivshar[1]

[1]*Nonlinear Physics Centre and Laser Physics Centre, Centre for Ultrahigh bandwidth Devices for Optical Systems (CUDOS), Research School of Physical Sciences and Engineering, Australian National University, Canberra, ACT 0200, Australia*

[2]*DTU Fotonik, Department of Photonics Engineering, Technical University of Denmark, Ørsteds Plads 345V, DK-2800 Kgs., Lyngby, Denmark*

We demonstrate, both theoretically and experimentally, the existence of nonlocal gap solitons in two-dimensional periodic photonic structures with defocusing thermal nonlinearity. We employ liquid-infiltrated photonic crystal fibers and show how the system geometry can modify the effective response of a nonlocal medium and the properties of two-dimensional gap solitons.

OCIS codes: 190.4420, 190.6135, 190.4870

The study of nonlinear wave propagation in periodic photonic structures has attracted a lot of recent interest due to possibility to engineer both linear and nonlinear properties of the material. In such systems, self-localized beams or lattice solitons can exist due to the interplay between effective diffraction and nonlinearity. Lattice solitons have been observed in various physical systems including optics [1], but only with on-site nonlinearity. The consideration of long-range nonlinear interactions between lattice sites, on the other hand, have shown to lead to novel nonlinear phenomena [2]. Such interactions appear when the nonlinear response at a particular lattice site is affected by the light intensity not only at this site but also at its neighbors. In periodic structures, long-range nonlinear interactions can naturally arise from nonlocal response. Nonlocality is common to many physical systems [3], occurring due to electrostatic interactions or diffusion processes, however, its effect in periodic structures has not been investigated experimentally.

In this Letter we study nonlinear localized states in a two-dimensional (2D) periodic system with nonlocal nonlinear interaction between the lattice sites and demonstrate, for the first time to our knowledge, the formation of *nonlocal gap solitons*. We utilize the hexagonal

lattice of the cladding of a photonic crystal fiber (PCF), where the holes are infiltrated with a high-index weakly absorbing oil. The nonlinearity in our system is *defocusing* and has thermal origin that arises due to the negative thermooptic coefficient of the oil, while the nonlocality originates from the diffusive nature of heat transfer [4].

Nonlocal solitons have been experimentally studied in homogeneous media [5], but in periodic structures only theoretical studies in the one-dimensional (1D) case can be found [6–9]. In defocusing materials, however, no nonlocal bright solitons have been observed to date. Only recently, it has been theoretically shown that 1D nonlocal solitons can exist in periodic structures with defocusing nonlinearity through localisation in the Bragg gap. In two dimensions, however, the situation can become dramatically different, since a complete Bragg gap only exists above a threshold value of the refractive index contrast [10, 11].

Therefore, we first study theoretically the existence of 2D nonlocal gap solitons in hexagonal lattices [11]. We consider the paraxial beam propagation in a periodic system with diffusive thermal nonlocal nonlinearity described by the equations,

$$\begin{aligned} ia_z(x,y,z) + \nabla_\perp^2 a(x,y,z) - p^2 a(x,y,z) \\ = -[n_0(x,y) - \tau(x,y,z) f(x,y)]^2 q^2 a(x,y,z), \end{aligned} \tag{1}$$

$$\nabla_\perp^2 \tau(x,y,z) = -|a(x,y,z)|^2, \tag{2}$$

where $a(x,y,z)$ stands for the normalized envelope of the electric field, and $\tau(x,y,z)$ is the normalized nonlinearly-induced temperature change. The transverse dimensions are scaled to the pitch Λ, which is the distance between two adjacent holes [Fig. 1(a)]. q is the normalized vacuum wavenumber, p is the normalized propagation constant, and $n_0(x,y)$ is the linear periodic refractive index. $f(x,y)$ is a normalized nonlinear coefficient with $f(x,y) = 1$ in the holes and zero elsewhere. This is justified since the thermal nonlinear response of the liquid dominates the thermal response of the glass. Due to our scaling $-\tau(x,y,z)f(x,y)$ can be interpreted as the light induced index change.

Our structure [Fig. 1(a)] consists of high-index cylinders placed in a hexagonal pattern inside a circle with radius $R_0 = 5\Lambda$. R_0 must be large enough to encompass all the high-index cylinders and our results do not depend on its value. Away from the core the electric field decays rapidly, and we can therefore assume that a vanishes at the boundary of our computational domain R_0. The boundary condition for the temperature field requires a more careful analysis since commercially available PCFs often contain a large homogeneous region of silica outside the last ring of holes. If we assume that the physical fiber has a radius $R_1 = sR_0$ ($s \geq 1$), and that the temperature at the outer boundary is constant, $\tau(r = sR_0/\Lambda) = 0$, it can be shown that $\tau(R_0/\Lambda)/\tau_r(R_0/\Lambda) = -\log(s)R_0/\Lambda$. Here τ_r denotes differentiation with respect to radial coordinate. The above relation is derived under the condition that the heat distribution in the region from R_0 to R_1 is radially symmetric, and that there is no heat

source in this region. The meaning of this relation is that one can practically control the electric field inside the lattice by varying the homogeneous spatial extent of the fibre (where the field is zero). This is a clear signature of the nonlocal thermal response, where the degree of nonlocality in the system is measured by the parameter $s = R_1/R_0$. The larger s relates to stronger nonlocality.

The 2D lattice with thermal nonlinearity is inherently finite because the nonlinearity relies on the boundaries [4]. Therefore, we find the eigenmodes of Eq. (1) on the finite domain shown in Fig. 1(a). The discrete spectrum of eigenvalues is divided into bands of closely spaced values separated by large jumps, similarly to the Bloch states of an infinite periodic lattice as shown in Fig. 1(b) ($d/\Lambda = 0.5$). In these calculations $n(x, y) = 1.4605$ in the holes, and 1.46 elsewhere. A bandgap is seen to open up at $q \approx 140$. In Fig. 1(b) the edges of the first finite bandgap of the corresponding infinite periodic lattice are also plotted with solid lines. At large q the edges of the first gap for the finite and the infinite structure almost coincide, while at smaller values there are propagation constants where a gap exists in the infinite, but does not exist in the finite structure.

The presence of the bandgap allows for existence of nonlinear localized states which for defocusing nonlinearity bifurcate from the bottom of the first band. We find these modes by looking for self-consistent z-independent solutions of Eqs. (1-2). Importantly, our calculations presented in Fig. 2 show that the gap solitons occupy the whole bandgap, regardless of the degree of nonlocality. We have tested this for different relative hole-diameters and outer boundaries, and every time the gap solitons occupy the whole bandgap. This is in contrast to earlier studies of asymmetric nonlocal response where solitons cease to exist at large nonlocality [7].

In Fig. 2(a), we show the soliton power vs. effective index for different values of nonlocality s. Notice that at high powers even solitons with propagation constants inside the second band of the corresponding linear structure exist. This apparent contradiction is a result of the finite size of our system which enables the temperature response to perturb the whole lattice, and thereby change the linear dispersion bands. The same behavior was also recently reported for a 1D system [9]. Another interesting feature seen in Fig. 2(a) is the decrease of the soliton power at increased degree of nonlocality. This is somewhat counter-intuitive, as one might expect that with increase of the thermal mass of the fibre (larger s) one would need to inject more power in order to achieve the same nonlinear effect.

In Fig. 2(b) we plot the soliton width $w_a = (\int r^2|a|^2 dxdy / \int |a|^2 dxdy)^{1/2}$ as a function of $n_{\text{Eff}} = p/q$ for different values of the nonlocality parameter s. The solitons are seen to localize as they move further into the bandgap, until the effective index reaches approximately the middle of the bandgap. Then the solitons start to delocalize again. This behavior is similar to what has been observed for gap solitons with local nonlinearity [13]. The main effect of

nonlocality in the system is the spatial broadening of the solitons with increasing parameter s. This behavior is typical to other nonlocal nonlinear systems [3].

An example of a gap-soliton profile is shown in Fig. 3(a). An inherent signature of the localization in the Bragg gap is the staggered phase structure shown in Fig. 3(b). This staggered structure is in the form of concentric rings around the central hole and resembles the electric field profile of one-dimensional gap solitons [12]. An important difference from gap solitons with local nonlinearity is the actual induced index change. In the thermal nonlocal case, this is represented by the induced temperature response [Fig. 3(d)] that is extended fully towards the boundaries of the structure.

To verify experimentally our predictions that gap solitons exists in nonlocal 2D lattice, we employ a system comprising the liquid-infiltrated PCF cladding, similar to our earlier experiments [14]. We use a commercially available fibre LMA-15 (Crystal Fibre) with a relative hole diameter $d/\Lambda \approx 0.498$ and $s \approx 1$. The cladding holes are filled by capillary action with an index matching oil ($n = 1.48$). The fibre is placed in a temperature controlled oven and heated to 76°C such that the refractive index of the oil is reduced closer to the index of silica. 532 nm light is butt coupled into a single infiltrated hole in the cladding, well away from the core, using a single-mode fibre. In this system, we observe linear diffraction at low input power (~ 3 mW) [Fig. 4(a)], corresponding to propagation of approximately three diffraction lengths. At high laser power (~ 100 mW) [Fig. 4(b)] we observe nonlinear self-localization to almost a single lattice site. Utilizing a pinhole we also measure the amount of light in the input hole as a function of the power injected in the fibre [Fig. 4(c)]. This dependence effectively represents the degree of localization achieved experimentally, and it corresponds to the theoretical predictions in Fig. 2. Indeed, our experiments confirm that the amount of localization is highest for intermediate powers, while the soliton is delocalised at both band edges. In addition, we observe the alternating phase structure of the gap solitons by producing an interference of the nonlinear mode [Fig. 4(b)] and a wide inclined reference beam. In the resulting interferogram [Fig. 4(d)], the input hole is out of phase with the first ring (upper line, expressed in a half-a-period shift in the interference fringes), while the first ring has constant phase (lower line).

It is important to mention that in our previous experiments [14] utilising infiltrated fibers with stronger nonlocality $s \approx 2$, we observed no localization but only beam defocusing. This is a direct consequence of the fact that the nonlocal solitons in those fibers are much wider (due to the larger degree of nonlocality) and therefore they could not be excited via single site coupling. In this presented work our nonlocal parameter is $s = 1$. Hence the observed localization is an indication of the formation of nonlocal gap solitons.

In conclusion, we have studied theoretically and generated in experiment nonlocal gap solitons in liquid-infiltrated photonic-crystal fibers. We have shown a possibility to control

nonlocality in a realistic periodic structure by varying its boundaries.

PDR thanks the Australian National University for hospitality. The work was supported by the Australian Research Council through Center of Excellence program. We thank A. Bjarklev for help with fiber selection.

References

1. H. S. Eisenberg, Y. Silberberg, R. Morandotti, A. R. Boyd, and J. S. Aitchison, "Discrete Spatial Optical Solitons in Waveguide Arrays," Phys. Rev. Lett. **81**, 3383 (1998).
2. S. F. Mingaleev, Yu, S. Kivshar, and R. A. Sammut, "Long-range interaction and nonlinear localized modes in photonic crystal waveguides," Phys. Rev. E **62**, 5777 (2000).
3. W. Krolikowski, O. Bang, N. I. Nikolov, D. Neshev, J. Wyller, J. J. Rasmussen, and D. Edmundson, "Modulational instability, solitons and beam propagation in spatially nonlocal nonlinear media," J. Opt. B **6**, S288 (2004).
4. A. Minovich, D. N. Neshev, A. Dreischuh, W. Krolikowski, and Yu. S. Kivshar, "Experimental reconstruction of nonlocal response of thermal nonlinear optical media," Opt. Lett. **32**, 1599 (2007).
5. C. Rotschild, B. Alfassi, O. Cohen, and M. Segev, "Long-range interactions between optical solitons," Nat. Phys. **2**, 769 (2006).
6. Z. Xu, Y. V. Kartashov, and L, Torner, "Soliton Mobility in Nonlocal Optical Lattices," Phys. Rev. Lett. **95**, 113901 (2005).
7. Z. Xu, Y. V. Kartashov, and L. Torner, "Gap solitons supported by optical lattices in photorefractive crystals with asymmetric nonlocality," Opt. Lett. **31**, 2027 (2006).
8. Y.-Y. Lin, I-H. Chen, and R.-K. Lee, "Breather-like collision of gap solitons in Bragg gap regions within nonlocal nonlinear photonic crystal," J. Opt. A: Pure Appl. Opt. **10**, 044017 (2008).
9. N. K. Efremidis, "Nonlocal lattice solitons in thermal media," Phys. Rev. A **77**, 063824 (2008).
10. J. W. Fleischer, M. Segev, N. K. Efremidis, and D. N. Christodoulides, "Observation of two-dimensional discrete solitons in optically induced nonlinear photonic lattices," Nature **422,** 147 (2003).
11. C. R. Rosberg, D. N. Neshev, A. A. Sukhorukov, W. Krolikowski, and Yu. S. Kivshar, "Observation of nonlinear self-trapping in triangular photonic lattices," Opt. Lett. **32**, 397 (2007).
12. Yu. S. Kivshar, "Self-localization in arrays of defocusing wave-guides," Opt. Lett. **18,** 1147 (1993).
13. P. J. Y. Louis, E. A. Ostrovskaya, C. M. Savage, and Yu. S. Kivshar, "Bose-Einstein condensates in optical lattices: Band-gap structure and solitons," Phys. Rev. A **67**, 013602 (2003).
14. C. R. Rosberg, F. H. Bennet, D. N. Neshev, W. Krolikowski, Yu. S. Kivshar, P. D. Rasmussen, O. Bang, and A. Bjarklev, "Tunable diffraction and self-defocusing in liquid-filled photonic crystal fibers," Opt. Express **15**, 12145 (2007).

Figure Captions

Fig. 1. (Color online) (a) System geometry. (b) Bandgap structure for $n_S = 1.46$, $n_L = 1.4605$, and $d/\Lambda = 0.5$. Shaded regions correspond to the bands of the finite structure in (a), while the solid lines show the edges of the first bandgap of an infinite lattice. The dashed line indicates the index of the solid material n_S.

Fig. 2. (Color online) Families of nonlocal gap solitons. (a,b) Power $P = \int |E|^2 dr$ and soliton width vs. effective index for different values of s. The normalized wave number is $q = 200$. The dots correspond to the example in Fig. 3.

Fig. 3. (Color online) Numerically calculated nonlocal gap soliton for power $P = 4{\cdot}10^{-5}$ and $s = 10$, marked with a dot in Fig. 2. (a) Intensity and (b) corresponding phase distribution. (c) Soliton profile and (d) induced temperature change along the symmetry line shown white dashed line in (a).

Fig. 4. (Color online) (a, b) Experimentally observed output diffraction pattern and soliton localisation in a liquid infiltrated PCF, at low and high input power, respectively. (c) Fraction of light in the input hole vs. input power. (d) Measured interference pattern of the output beam with an inclined reference beam.

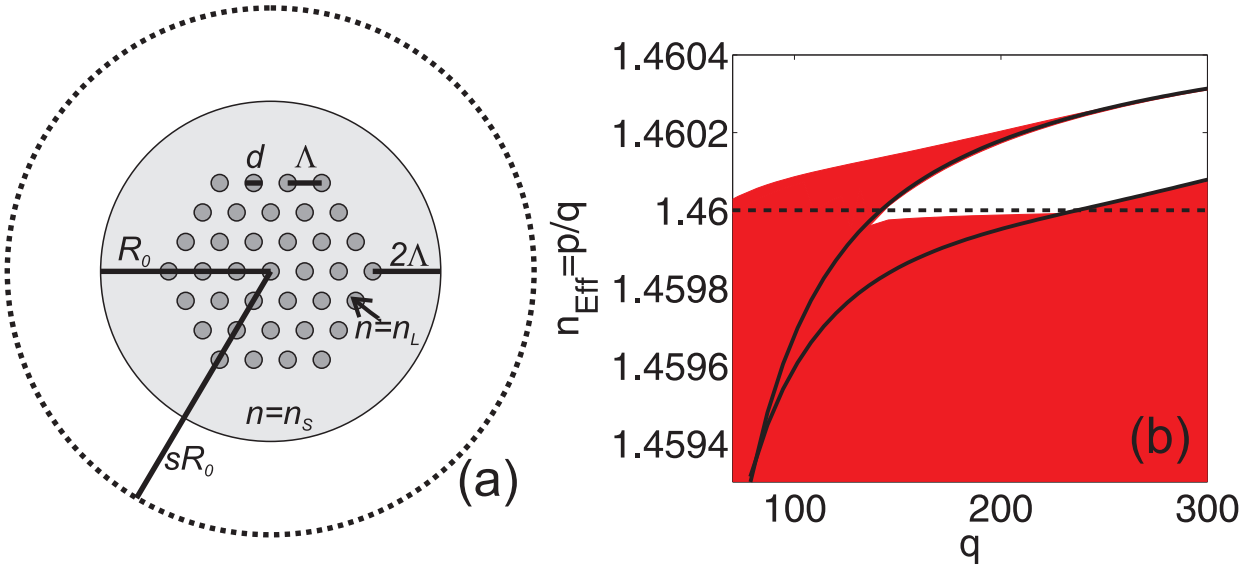

Fig. 1. (Color online) (a) System geometry. (b) Bandgap structure for $n_S = 1.46$, $n_L = 1.4605$, and $d/\Lambda = 0.5$. Shaded regions correspond to the bands of the finite structure in (a), while the solid lines show the edges of the first bandgap of an infinite lattice. The dashed line indicates the index of the solid material n_S.

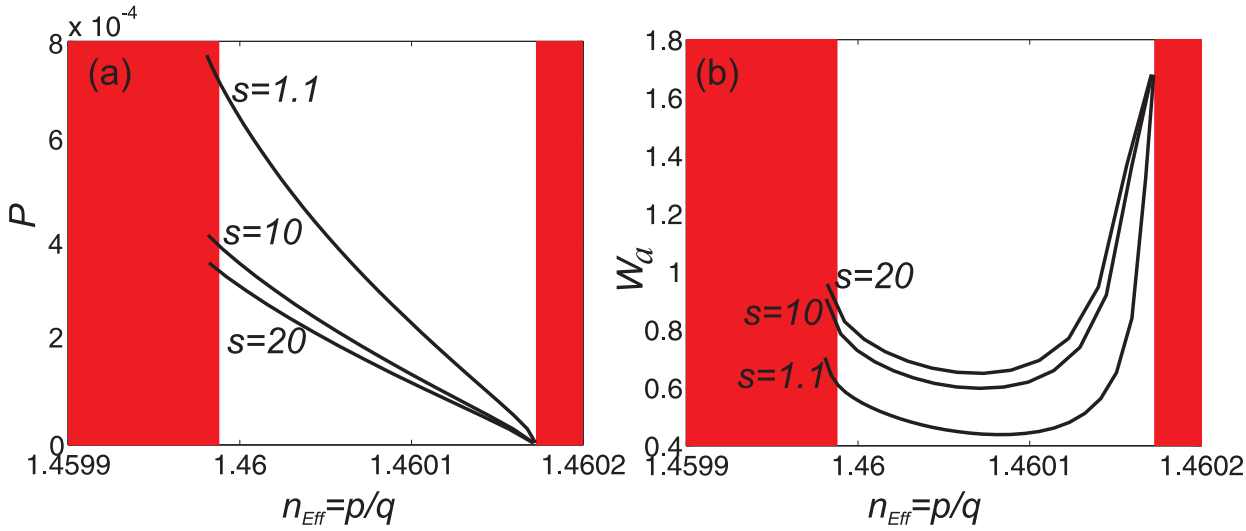

Fig. 2. (Color online) Families of nonlocal gap solitons. (a,b) Power $P = \int |E|^2 dr$ and soliton width vs. effective index for different values of s. The normalized wave number is $q = 200$. The dots correspond to the example in Fig. 3.

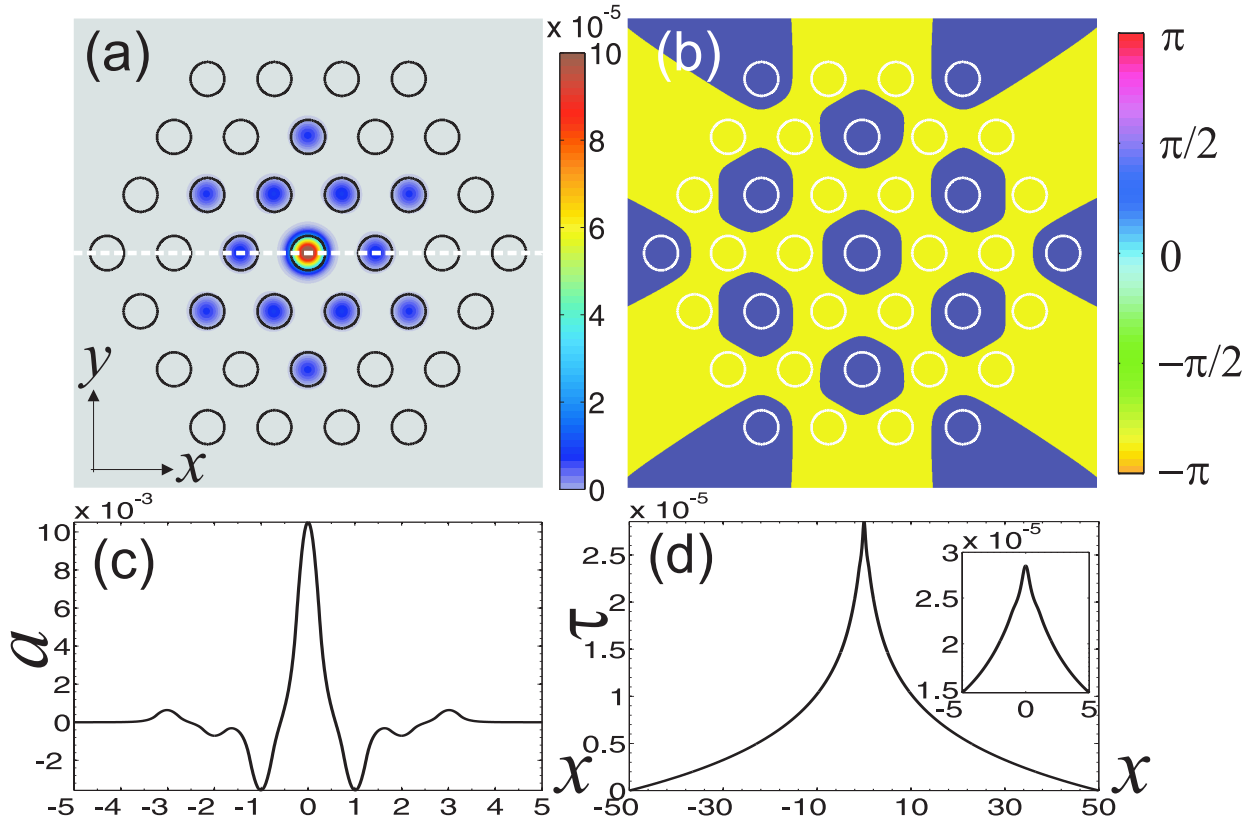

Fig. 3. (Color online) Numerically calculated nonlocal gap soliton for power $P = 4 \cdot 10^{-5}$ and $s = 10$, marked with a dot in Fig. 2. (a) Intensity and (b) corresponding phase distribution. (c) Soliton profile and (d) induced temperature change along the symmetry line shown white dashed line in (a).

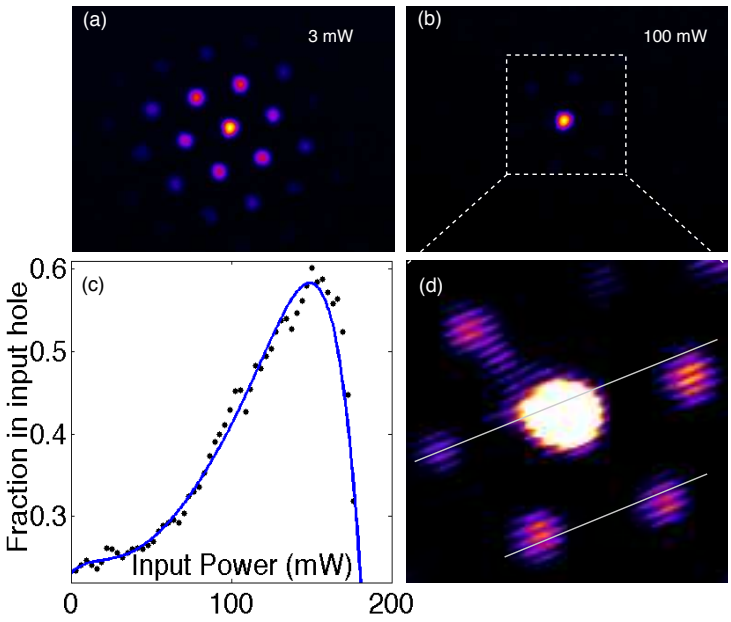

Fig. 4. (Color online) (a, b) Experimentally observed output diffraction pattern and soliton localisation in a liquid infiltrated PCF, at low and high input power, respectively. (c) Fraction of light in the input hole vs. input power. (d) Measured interference pattern of the output beam with an inclined reference beam.